INTERNATIONAL JOURNAL FOR NUMERICAL METHODS IN FLUIDS, VOL. 9, 1487–1501 (1989)

A FINITE ELEMENT ANALYSIS OF LAMINAR UNSTEADY FLOW OF VISCOELASTIC FLUIDS THROUGH CHANNELS WITH NON-UNIFORM CROSS-SECTIONS

R. PONNALAGARSAMY AND M. KAWAHARA

Department of Civil Engineering, Chuo University, Kasuga, 1-13-27, Bunkyo-ku, Tokyo 112, Japan

SUMMARY

The effects of non-Newtonian behaviour of a fluid and unsteadiness on flow in a channel with non-uniform cross-section have been investigated. The rheological behaviour of the fluid is assumed to be described by the constitutive equation of a viscoelastic fluid obeying the Oldroyd-B model. The finite element method is used to analyse the flow. The novel features of the present method are the adoption of the velocity correction technique for the momentum equations and of the two-step explicit scheme for the extra stress equations. This approach makes the computational scheme simple in algorithmic structure, which therefore implies that the present technique is capable of handling large-scale problems. The scheme is completed by the introduction of balancing tensor diffusivity (wherever necessary) in the momentum equations. It is important to mention that the proper boundary condition for pressure (at the outlet) has been developed to solve the pressure Poisson equation, and then the results for velocity, pressure and extra stress fields have been computed for different values of the Weissenberg number, viscosity due to elasticity, etc. Finally, it is pertinent to point out that the present numerical scheme, along with the proper boundary condition for pressure developed here, demonstrates its versatility and suitability for analysing the unsteady flow of viscoelastic fluid through a channel with non-uniform cross-section.

KEY WORDS Viscoelastic fluid Polymer flow Velocity correction method Two-step explicit scheme Pressure boundary condition

INTRODUCTION

The interest expressed in the unsteady flow of viscoelastic fluid through abrupt expansions or contractions and other geometries such as converging–diverging channels is primarily due to the wide range of applications in the understanding of idealized industrial problems and the fundamental understanding of cardiovascular diseases. Further, the computation and numerical simulation of such problems, as well as an understanding of the underlying mathematical features of the equations used to model them, are very important for evaluating the consequences of choosing a particular constitutive theory and for analysing the resulting performance of the model in relation to experiments. In view of this, many investigators have developed numerous numerical methods to analyse the flow of viscoelastic fluid through a complicated geometry and obtained significant progress in marrying theory and experiment, at least as far as qualitative features of the flow are concerned. However, it must be admitted that severe problems remain and numerical simulation has been unable to meet many challenges posed in the experimental observations of the

0271–2091/89/121487–15$07.50 *Received September 1988*

flow. It is well known that one of the major unsolved problems in the numerical simulation of viscoelastic fluid flow is the breakdown of numerical algorithms even for modest values of the elasticity parameter. The possible causes of the breakdown have been attributed to the unsuitability of certain constitutive models, change of type of the governing equations, bifurcation phenomena, etc. as the Weissenberg number increases and the interaction between discretization error and non-linear iteration, none of them being final at the present time. However, in many ways the problem is still an open one in urgent need of attention. Hence, with a view to developing or improving the numerical technique to meet this difficulty and understanding idealized industrial chemical and polymer processes (with the aim of aiding in the design of such processes and the apparatus required to control or alter the polymer and chemical processes in a more precise way), a modest effort is made in the present analysis to investigate the unsteady flow of viscoelastic fluid and to check the suitability of the present numerical technique.

The basic idea of the velocity correction method was originally presented by Chorin[1] for a finite difference scheme. Donea *et al.*,[2,3] Schneider and Raithby,[4] Glowinsky *et al.*[5] and Kawahara and Ohmiya[6] have adapted the idea to the finite element method. Ramaswamy *et al.*[7] have developed the Lagrangian finite element method in which they used the velocity correction technique to solve problems involving the sloshing dynamics of viscous fluids. Ramaswamy[8] has analysed various flow models using the velocity correction method. In all these investigations[1-8] the rheology of the fluid is assumed to be Newtonian, but the boundary condition for pressure to solve the pressure Poisson equation is somewhat unclear. It is worthwhile to mention that the applicability of problems assuming the fluid as Newtonian is very limited in chemical and polymer industrial problems as well as in biological fluid flow problems, and choosing the proper boundary condition for pressure, especially at the outlet, is also important in understanding the flow phenomena more or less exactly. It is therefore pertinent to investigate the flow of non-Newtonian fluid with the proper boundary condition for pressure at an outlet with an open boundary.

The two-dimensional flow of viscoelastic fluid has been studied by several research groups with mixed results.[9] Josse and Finlayson[10] have simulated the flow of a co-deformational Maxwell fluid using the finite element method and analysed the variation of only axial extra stress along the centreline for different values of Weissenberg number. A new algorithm for the solution of the set of differential equations governing the flow of viscoelastic fluid has been proposed without computational results by Townsend and Webster.[11] Crochet and Marchal[12] have numerically simulated the steady flows of viscoelastic fluids (Maxwell and Oldroyd-B models) and illustrated the results in the form of streamlines for various values of the Deborah number. A numerical method for solving time-dependent problems in one space variable for the Oldroyd-B model has been provided by Townsend[13] as a first step. Song and Yoo[14] have performed a numerical simulation of the flow of an upper convected Maxwell fluid through planar 4:1 contraction and pointed out that as the Weissenberg number increases, the streamlines become flatter in the upstream region of contraction. Yoo and Joseph[15] considered the same flow through a channel with wavy walls. It is of interest to point out here that the unsteady two-dimensional flow of viscoelastic fluid obeying the Oldroyd-B model, using the finite element technique in which the computational scheme is simple in algorithmic structure and cost-effective, has not been simulated numerically for the case of an open boundary at the outlet. Further, many investigators have presented the computational results in terms of streamfunction/vorticity rather than in terms of the primitive variables such as velocity, pressure and extra stress fields. In view of this, it is of interest to investigate the effects of unsteadiness and the non-Newtonian nature of the fluid (Oldroyd-B model) simultaneously on the flow using the present numerical scheme with the proper boundary condition for pressure to solve the pressure Poisson equation.

BASIC EQUATIONS

We consider a two-dimensional, unsteady, laminar, fully developed flow of viscoelastic fluid through channels with non-uniform cross-sections as shown in Figures 1 and 2. The equations governing the flow are (in dimensionless form) as follows:

equation of continuity

$$\frac{\partial u}{\partial x}+\frac{\partial v}{\partial y}=0; \tag{1}$$

momentum equations in x- and y-directions

$$\frac{\partial u}{\partial t}+u\frac{\partial u}{\partial x}+v\frac{\partial u}{\partial y}=-\frac{\partial p}{\partial x}+\frac{\mu_2}{Re}\left(\frac{\partial^2 u}{\partial x^2}+\frac{\partial^2 u}{\partial y^2}\right)+\frac{\partial T_{xx}}{\partial x}+\frac{\partial T_{xy}}{\partial y}, \tag{2}$$

$$\frac{\partial v}{\partial t}+u\frac{\partial v}{\partial x}+v\frac{\partial v}{\partial y}=-\frac{\partial p}{\partial y}+\frac{\mu_2}{Re}\left(\frac{\partial^2 v}{\partial x^2}+\frac{\partial^2 v}{\partial y^2}\right)+\frac{\partial T_{xy}}{\partial x}+\frac{\partial T_{yy}}{\partial y}; \tag{3}$$

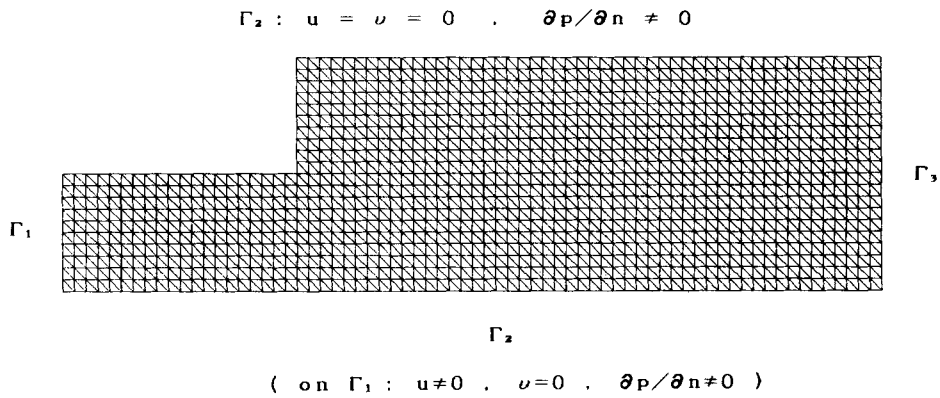

Figure 1. Geometry of channel with abrupt expansion

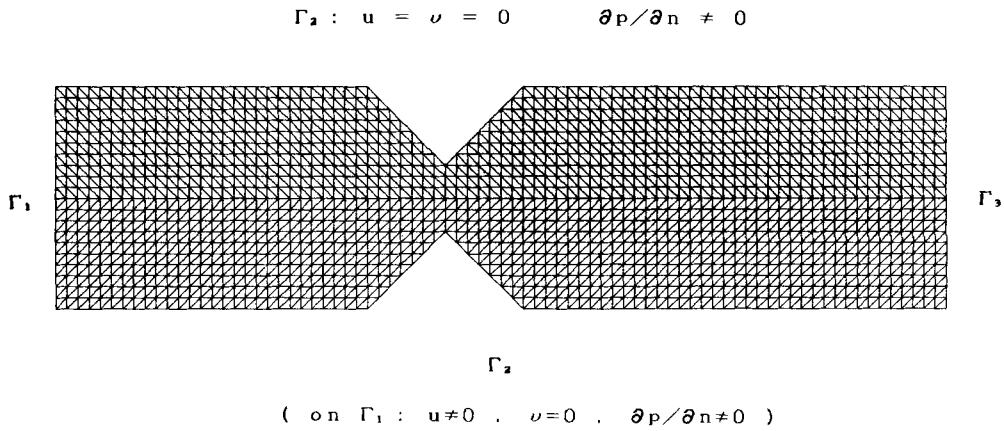

Figure 2. Geometry of converging–diverging channel

extra stresses (for Oldroyd-B model)

$$\lambda We\frac{\partial T_{xx}}{\partial t}=\left(\frac{2\mu_1}{Re}\right)\frac{\partial u}{\partial x}-T_{xx}-\lambda We\left(u\frac{\partial T_{xx}}{\partial x}+v\frac{\partial T_{xx}}{\partial y}\right)+2\lambda We\left(T_{xx}\frac{\partial u}{\partial x}+T_{xy}\frac{\partial u}{\partial y}\right), \tag{4}$$

$$\lambda We\frac{\partial T_{xy}}{\partial t}=\frac{\mu_1}{Re}\left(\frac{\partial u}{\partial y}+\frac{\partial v}{\partial x}\right)-T_{xy}-\lambda We\left(u\frac{\partial T_{xy}}{\partial x}+v\frac{\partial T_{xy}}{\partial y}\right)+\lambda We\left(T_{xx}\frac{\partial v}{\partial x}+T_{yy}\frac{\partial u}{\partial y}\right), \tag{5}$$

$$\lambda We\frac{\partial T_{yy}}{\partial t}=\left(2\frac{\mu_1}{Re}\right)\frac{\partial v}{\partial y}-T_{yy}-\lambda We\left(u\frac{\partial T_{yy}}{\partial x}+v\frac{\partial T_{yy}}{\partial y}\right)+2\lambda We\left(T_{yy}\frac{\partial v}{\partial y}+T_{xy}\frac{\partial v}{\partial x}\right); \tag{6}$$

where u and v are the velocities in the axial (x) and vertical (y) directions, p is the pressure, t is the time, $\mu_2(=\hat{\mu}_2/\hat{\mu}_s)$ is the viscosity, $\hat{\mu}_2$ is the shear viscosity, $\hat{\mu}_s$ is the standard viscosity (Newtonian), $Re(=\hat{\rho}\hat{U}_0\hat{L}_0/\hat{\mu}_s)$ is the Reynolds number, $\hat{\rho}$ is the density, $\hat{U}_0$ is the characteristic velocity, $\hat{L}_0$ is the characteristic length, T_{xx}, T_{xy} and T_{yy} are the extra stresses, λ is the relaxation time, We $(=\hat{U}_0\hat{\lambda}_s/\hat{L}_0)$ is the Weissenberg number, $\hat{\lambda}_s$ is the standard elastic time constant and $\mu_1(=\hat{\mu}_1/\hat{\mu}_s)$ is the viscosity due to elasticity. ($\hat{}$ over a letter denotes the dimensional form of the corresponding quantity.) The dimensionless retardation time may be obtained from the following relation:

$$\lambda_1=\lambda\mu_2/(\mu_1+\mu_2). \tag{7}$$

The boundary conditions (Dirichlet) are

$$u=\bar{u}(y,t),\quad v=0,\quad T_{xx}=\bar{T}_{xx}(y,t),\quad T_{xy}=\bar{T}_{xy}(y,t),\quad T_{yy}=0\quad \text{on } \Gamma_1, \tag{8}$$

$$u=v=0\quad \text{on } \Gamma_2, \tag{9}$$

and on Γ_3, u, v, T_{xx}, T_{xy} and T_{yy} are unknown. The terms $\bar{u}$, $\bar{T}_{xx}$ and $\bar{T}_{xy}$ are known functions. The entire boundary Γ is expressed as

$$\Gamma=\Gamma_1\cup\Gamma_2\cup\Gamma_3\quad \text{with } \Gamma_1\cap\Gamma_2\cap\Gamma_3. \tag{10}$$

For the entire (whole) solution domain, the initial conditions ($t=0$) are

$$u=\bar{u}_0(x,y),\quad v=\bar{v}_0(x,y),\quad T_{xx}=\bar{T}_{xx0}(x,y),$$
$$T_{xy}=\bar{T}_{xy0}(x,y),\quad T_{yy}=\bar{T}_{yy0}(x,y)\quad \text{with}\quad \frac{\partial\bar{u}_0}{\partial x}+\frac{\partial\bar{v}_0}{\partial y}=0. \tag{11}$$

FINITE ELEMENT FORMULATION

Employing the purely explicit Euler first-order scheme in time integration, the velocity correction method and the Galerkin method for space discretization, equations (2) and (3) are transformed to a set of non-linear simultaneous equations as follows:

Intermediate velocity field

$$\bar{\mathbf{M}}_{\alpha\beta}\tilde{\mathbf{u}}_\beta^{n+1}=\bar{\mathbf{M}}_{\alpha\beta}\mathbf{u}_\beta^n-\Delta t\left(\frac{\mu_2}{Re}\mathbf{S}_{\alpha\beta}\mathbf{u}_\beta^n+\frac{\mu_2}{Re}\mathbf{C}_u^n-\mathbf{A}_{\alpha\beta}\mathbf{u}_\beta^n+\mathbf{R}_{\alpha\beta}^x\mathbf{T}_{xx\beta}^n+\mathbf{R}_{\alpha\beta}^y\mathbf{T}_{xy\beta}^n\right), \tag{12}$$

$$\bar{\mathbf{M}}_{\alpha\beta}\tilde{\mathbf{v}}_\beta^{n+1}=\bar{\mathbf{M}}_{\alpha\beta}\mathbf{v}_\beta^n-\Delta t\left(\frac{\mu_2}{Re}\mathbf{S}_{\alpha\beta}\mathbf{v}_\beta^n+\frac{\mu_2}{Re}\mathbf{C}_v^n-\mathbf{A}_{\alpha\beta}\mathbf{v}_\beta^n+\mathbf{R}_{\alpha\beta}^x\mathbf{T}_{xy\beta}^n+\mathbf{R}_{\alpha\beta}^y\mathbf{T}_{yy\beta}^n\right); \tag{13}$$

pressure Poisson equation

$$\mathbf{S}_{\alpha\beta}\mathbf{p}_\beta^n = \mathbf{C}_p^n - (1{\cdot}0/\Delta t)\,(\mathbf{R}_{\alpha\beta}^x \tilde{\mathbf{u}}_\beta^{n+1} + \mathbf{R}_{\alpha\beta}^y \tilde{\mathbf{v}}_\beta^{n+1}); \tag{14}$$

exact velocty field

$$\bar{\mathbf{M}}_{\alpha\beta}\mathbf{u}_\beta^{n+1} = \bar{\mathbf{M}}_{\alpha\beta}\tilde{\mathbf{u}}_\beta^{n+1} - \Delta t\,\mathbf{R}_{\alpha\beta}^x \mathbf{p}_\beta^n, \tag{15}$$

$$\bar{\mathbf{M}}_{\alpha\beta}\mathbf{v}_\beta^{n+1} = \bar{\mathbf{M}}_{\alpha\beta}\tilde{\mathbf{v}}_\beta^{n+1} - \Delta t\,\mathbf{R}_{\alpha\beta}^y \mathbf{p}_\beta^n; \tag{16}$$

where

$$\mathbf{M}_{\alpha\beta} = \int\int \mathbf{N}_\alpha \mathbf{N}_\beta \mathrm{d}x\mathrm{d}y,$$

$$\mathbf{S}_{\alpha\beta} = \int\int \left(\frac{\partial \mathbf{N}_\alpha}{\partial x}\frac{\partial \mathbf{N}_\beta}{\partial x} + \frac{\partial \mathbf{N}_\alpha}{\partial y}\frac{\partial \mathbf{N}_\beta}{\partial y}\right)\mathrm{d}x\mathrm{d}y,$$

$$\mathbf{A}_{\alpha\beta} = \int\int \mathbf{N}_\alpha \left(\mathbf{u}_\beta^{n\mathrm{T}}\mathbf{N}_\beta \frac{\partial \mathbf{N}_\beta}{\partial x} + \mathbf{v}_\beta^{n\mathrm{T}}\mathbf{N}_\beta \frac{\partial \mathbf{N}_\beta}{\partial y}\right)\mathrm{d}x\mathrm{d}y,$$

$$\mathbf{R}_{\alpha\beta}^x = \int\int \mathbf{N}_\alpha \frac{\partial \mathbf{N}_\beta}{\partial x}\mathrm{d}x\mathrm{d}y,$$

$$\mathbf{R}_{\alpha\beta}^y = \int\int \mathbf{N}_\alpha \frac{\partial \mathbf{N}_\beta}{\partial y}\mathrm{d}x\mathrm{d}y,$$

the superscripts n and $n+1$ indicate the corresponding values at the nth and $(n+1)$th time steps respectively, $\mathbf{C}_u^n$, $\mathbf{C}_v^n$ and $\mathbf{C}_p^n$ are the vectors of natural (Neumann) boundary conditions for the velocities and pressure respectively, $\mathbf{N}$ denotes an interpolation function and $\bar{\mathbf{M}}_{\alpha\beta}$ is the lumped mass matrix obtained simply by summing across each row of the consistent mass matrix $\mathbf{M}_{\alpha\beta}$ and placing the results on the diagonal. In the present analysis, linear interpolation functions based on the three-node triangular element are employed. Hence $\mathbf{N}_\alpha^{\mathrm{T}} = (N_1, N_2, N_3)$ is the vector of the basis function.

Utilizing the Galerkin method and the selective-lumping two-step explicit scheme for the numerical integration in time, the finite element equations for extra stress $\mathbf{T}_{xx}$ are obtained from equation (4) as follows.

For the first step,

$$\bar{\mathbf{M}}_{\alpha\beta}\mathbf{T}_{xx\beta}^{n+(1/2)} = \tilde{\mathbf{M}}_{\alpha\beta}\mathbf{T}_{xx\beta}^n + \frac{\Delta t}{2}\left(\frac{2\mu_1}{\lambda WeRe}\mathbf{R}_{\alpha\beta}^x \mathbf{u}_\beta^n - \frac{1}{\lambda We}\mathbf{M}_{\alpha\beta}\mathbf{T}_{xx\beta}^n - \mathbf{A}_{\alpha\beta}\mathbf{T}_{xx\beta}^n + \mathbf{E}_{\alpha\beta}^n \mathbf{u}_\beta^n + \mathbf{F}_{\alpha\beta}^n \mathbf{u}_\beta^n\right), \tag{17}$$

and for the second step,

$$\bar{\mathbf{M}}_{\alpha\beta}\mathbf{T}_{xx\beta}^{n+1} =$$

$$\tilde{\mathbf{M}}_{\alpha\beta}\mathbf{T}_{xx\beta}^n + \Delta t\left(\frac{2\mu_1}{\lambda WeRe}\mathbf{R}_{\alpha\beta}^x \mathbf{u}_\beta^n - \frac{1}{\lambda We}\mathbf{M}_{\alpha\beta}\mathbf{T}_{xx\beta}^{n+(1/2)} - \mathbf{A}_{\alpha\beta}\mathbf{T}_{xx\beta}^{n+(1/2)} + \mathbf{E}_{\alpha\beta}^{n+(1/2)}\mathbf{u}_\beta^n + \mathbf{F}_{\alpha\beta}^{n+(1/2)}\mathbf{u}_\beta^n\right), \tag{18}$$

where

$$\mathbf{E}^n_{\alpha\beta} = \iint \mathbf{N}_\alpha \left(\mathbf{T}^{nT}_{xx\beta} \mathbf{N}_\beta \frac{\partial \mathbf{N}_\beta}{\partial x} \right) \mathrm{d}x\mathrm{d}y,$$

$$\mathbf{F}^n_{\alpha\beta} = \iint \mathbf{N}_\alpha \left(\mathbf{T}^{nT}_{xy\beta} \mathbf{N}_\beta \frac{\partial \mathbf{N}_\beta}{\partial y} \right) \mathrm{d}x\mathrm{d}y$$

and the superscripts n, $n+1/2$ and $n+1$ indicate the corresponding values at the nth, $(n+1/2)$th and $(n+1)$th time steps respectively. In equations (17) and (18), $\tilde{\mathbf{M}}_{\alpha\beta}$ means the mixed coefficient, which is expressed as

$$\tilde{\mathbf{M}}_{\alpha\beta} = e\bar{\mathbf{M}}_{\alpha\beta} + (1-e)\mathbf{M}_{\alpha\beta}, \tag{19}$$

where e is known as the selective-lumping parameter. Similarly, the finite element equations for extra stresses $\mathbf{T}_{xy}$ and $\mathbf{T}_{yy}$ may be obtained from equations (5) and (6).

BOUNDARY CONDITIONS FOR PRESSURE

We have considered the boundary consisting of Γ_1 (inlet), Γ_2 (wall) and Γ_3 (outlet). It is of interest to mention that on Γ_1 and Γ_2 the Neumann (natural) boundary condition for the pressure, for the first time as far as the present flow problem is concerned, has been incorporated in equation (14) through the weak form of normal pressure gradient obtained from the momentum equations (2) and (3). A careful examination of equation (14) shows that to solve the pressure Poisson equation (PPE), in the Dirichlet (boundary) condition for pressure at least at one node must be prescribed because the matrix $\mathbf{S}_{\alpha\beta}$ is singular. Many investigators have numerically solved the Navier–Stokes equations and the flow of non-Newtonian fluids assuming that the value of pressure is equal to zero at the outlet (open boundary). Here we have used two types of boundary condition for solving the PPE. The first method is to compute the values of the tangential pressure gradient at all nodes, except one node at which the Dirichlet condition for pressure (for example, $p=0$) is prescribed, on the boundary Γ_3 by taking the weak form of the pressure gradient (over the surface) obtained from the tangential (vertical) component of the momentum equation (3). Knowing the pressure value ($p=0$) at the first nodal point, p_f, and the tangential pressure gradient at the second node, $(\partial p/\partial y)_s$ (neighbourhood of the first node on the open boundary Γ_3), the pressure value at the second nodal point, p_s, is computed from the formula

$$p_s = p_f + (\partial p/\partial y)_s (y_s - y_f), \tag{20}$$

where $y_s - y_f$ is the vertical distance between the second and first nodes. Similarly, we can compute the pressure values at all other nodal points on the open boundary using equation (20). The second method is to first obtain another pressure Poisson equation (called hereafter the PPEB) from the momentum equation (2) and (3) and the equation of continuity (1). The values of the pressure at all nodes along the open boundary Γ_3 have been computed by the weak form of the PPEB over the surface—which includes the boundary Γ_3 and its neighbourhood—using the known value of the pressure from the previous time step in the vicinity of the open boundary. Note that computing the value of the pressure gradient at the open boundary is not possible at the first time step by utilizing the weak form of the pressure gradient expression obtained from the tangential momentum equation (3), since although the velocities at the initial stage are known, those at the first time step are unknown. Thus it is not possible to compute the acceleration term $\partial v/\partial t$ at the first time step. This means that one cannot use the first method above to compute the pressure gradient at the open boundary for the first time step. In order to overcome this difficulty, we have adopted the following procedure. For the first time step we compute the value of the pressure at the open

boundary by the second method, while for the remaining time steps we use the first method. We can use the first method from the second time step onwards provided we assume that the value of the pressure is equal to zero at the open boundary for the first time step. Further, the value of the pressure at the open boundary may be taken to be the hydrostatic pressure value.

DISCUSSION

Flow of Oldroyd-B fluid through a channel with sudden expansion

For fixed values of Reynolds number ($Re = 10$) and relaxation time ($\lambda = 1{\cdot}0$), the velocity, pressure and extra stress fields have been computed with different values of solvent viscosity (μ_2), viscosity due to elasticity (μ_1) and Weissenberg number (We). The contours of the velocity, pressure and extra stress fields are illustrated in Figure (3–5) for different values of We and μ_1. At the outlet (open boundary) it is observed that an increase in μ_1 leads to a decrease in the axial velocity near the wall and an increase in its value near the centre of the outlet. The magnitude of

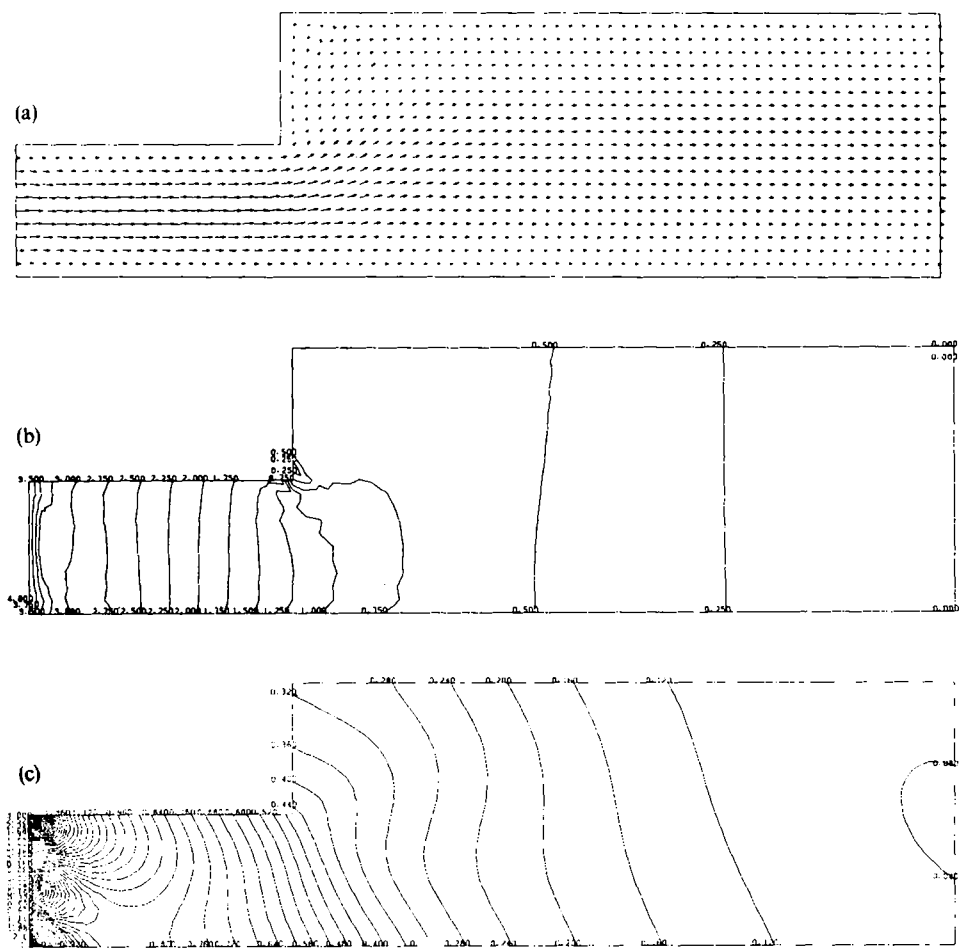

Fig. 3 (a–c)

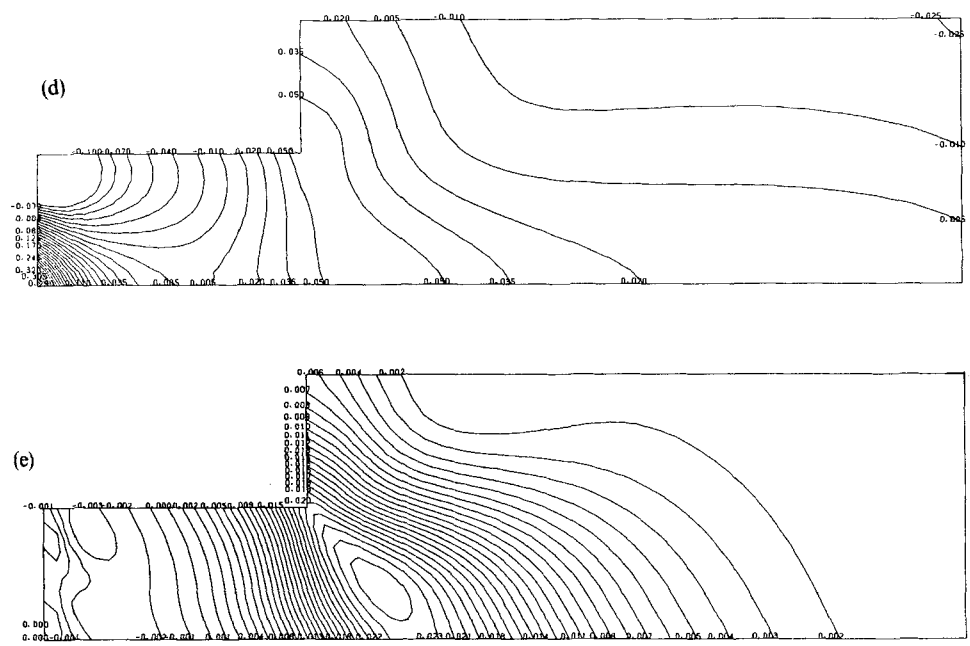

Figure 3. Contours of primitive variables for $Re = 10{\cdot}0$, $We = 1{\cdot}0$, $\mu_1 = 1{\cdot}0$, $\mu_2 = 1{\cdot}0$, $t = 4{\cdot}0$, $\lambda = 1{\cdot}0$: (a) velocity field; (b) pressure field; (c) extra stress T_{xx}; (d) extra stress T_{xy}; (e) extra stress T_{yy}

the vertical velocity also increases with an increase in μ_1. Similar behaviour of the axial velocity and opposite behaviour of the vertical velocity are seen as We or μ_2 increases.

The area and length of the back flow region decrease as μ_1 increases, but opposite behaviour is seen in the pressure drop between the inlet and outlet and in the magnitude of the extra stresses. The solvent viscosity shows a similar effect to μ_1, but its influence on the extra stresses is much less than that of μ_1. The area and length of the back flow region increase and the pressure drop and the magnitude of the extra stresses decrease as the ratio of the retardation time (λ_1) to the relaxation time (λ) increases. For the same value of the ratio λ_1/λ, the area and length of the back flow region, the pressure drop and the values of the extra stresses, for various values of μ_1 and μ_2 are quite different from each other, in contradiction to the previous observation. It seems that the individual characteristic values of the solvent viscosity and the viscosity due to elasticity play a crucial role in alteration of the area and length of the back flow region, the pressure drop and the extra stresses and that these flow characteristics are not significantly influenced by the ratio of the retardation time to the relaxation time for a fixed value of the relaxation time.

The variations of the extra stresses along the lower ($y = 0{\cdot}0$, $0{\cdot}0 \leqslant x \leqslant 7{\cdot}0$) and upper ($y = 2{\cdot}0$, $2{\cdot}0 \leqslant x \leqslant 7{\cdot}0$) walls of the channel for different values of We, μ_1 and μ_2 are tabulated in Tables I and II. Careful study of Tables I and II shows that the percentage decrease in the xx component of the extra stress (T_{xx}) along the lower and upper walls increases as the axial (x) distance increases for given values of We, μ_1 and μ_2. This percentage decrease in T_{xx} decreases insignificantly (or significantly) for a higher value of μ_1 or μ_2 (or We). For fixed values of We, μ_1 and μ_2 it is seen that the percentage decrease in T_{xy} along the lower and upper walls of the channel increases with an increase in x and its value is less (or more) for a higher value of We (or μ_1 and μ_2). Further, the variation of T_{yy} along the lower and upper walls is non-uniform and its magnitude increases as We or μ_1 increases.

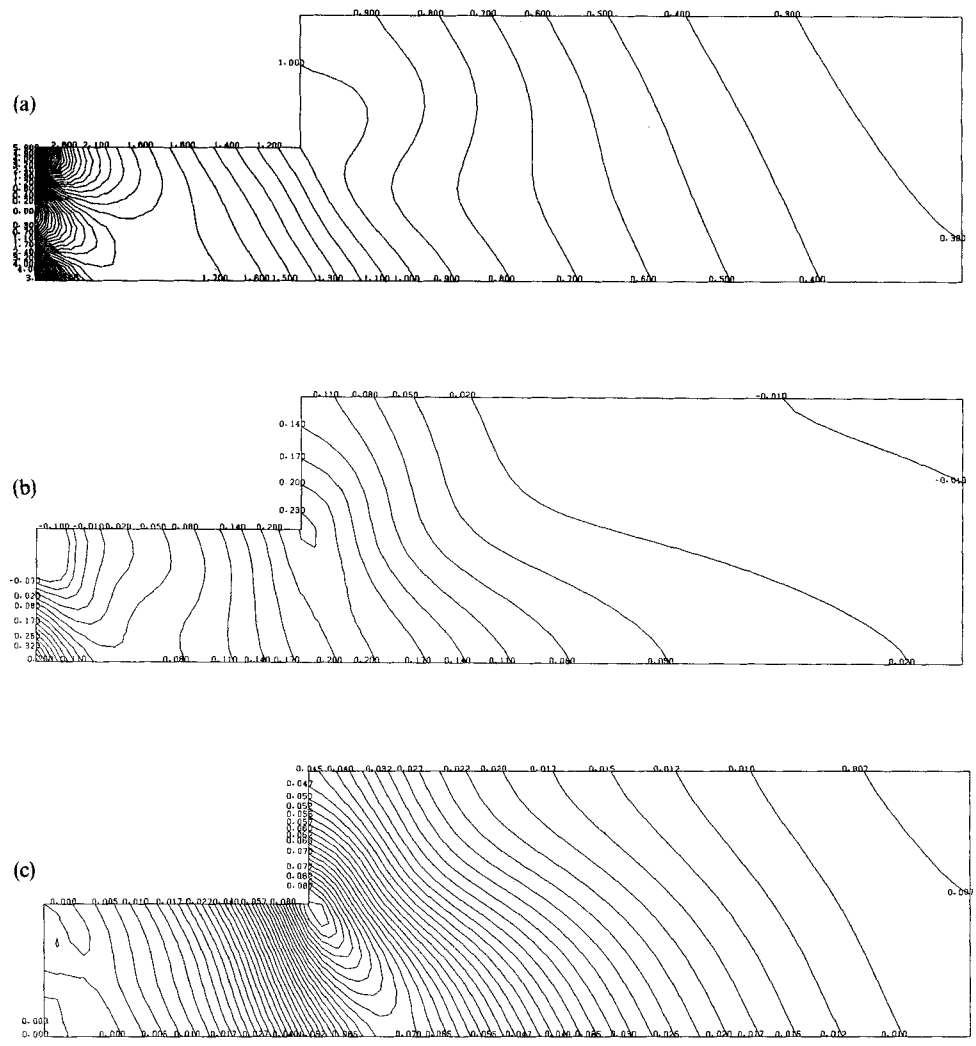

Figure 4. Distribution of extra stress field for $Re = 10{\cdot}0$, $We = 2{\cdot}0$, $\mu_1 = 1{\cdot}0$, $\mu_2 = 1{\cdot}0$, $t = 4{\cdot}0$, $\lambda = 1{\cdot}0$: (a) extra stress T_{xx}; (b) extra stress T_{xy}; (c) extra stress T_{yy}

Flow of Öldroyd-B fluid through a converging–diverging channel

In the present flow analysis, the balancing tensor diffusivity technique has been incorporated in the momentum equations. The extra stress distributions for $Re = 10{\cdot}0$, $We = 1{\cdot}0$, $\lambda = 1{\cdot}0$, $\mu_2 = 1{\cdot}0$ and $\mu_1 = 0{\cdot}5$ are shown in Figure 6. A study of these distributions shows that the extra stress T_{xx} along the walls decreases as one moves from the uniform flow region to the converging section and then increases in the converging region. Its value continues to increase in the diverging section of the channel and then decreases in the downstream. Similar behaviour is observed in the case of T_{xy}. Non-uniformity of the decrease or/and increase in T_{yy} along the walls is observed for given values of We, μ_1 and μ_2. Furthermore, the magnitude of T_{yy} is less than that of T_{xx} or T_{xy} (for the values of the parameters considered here).

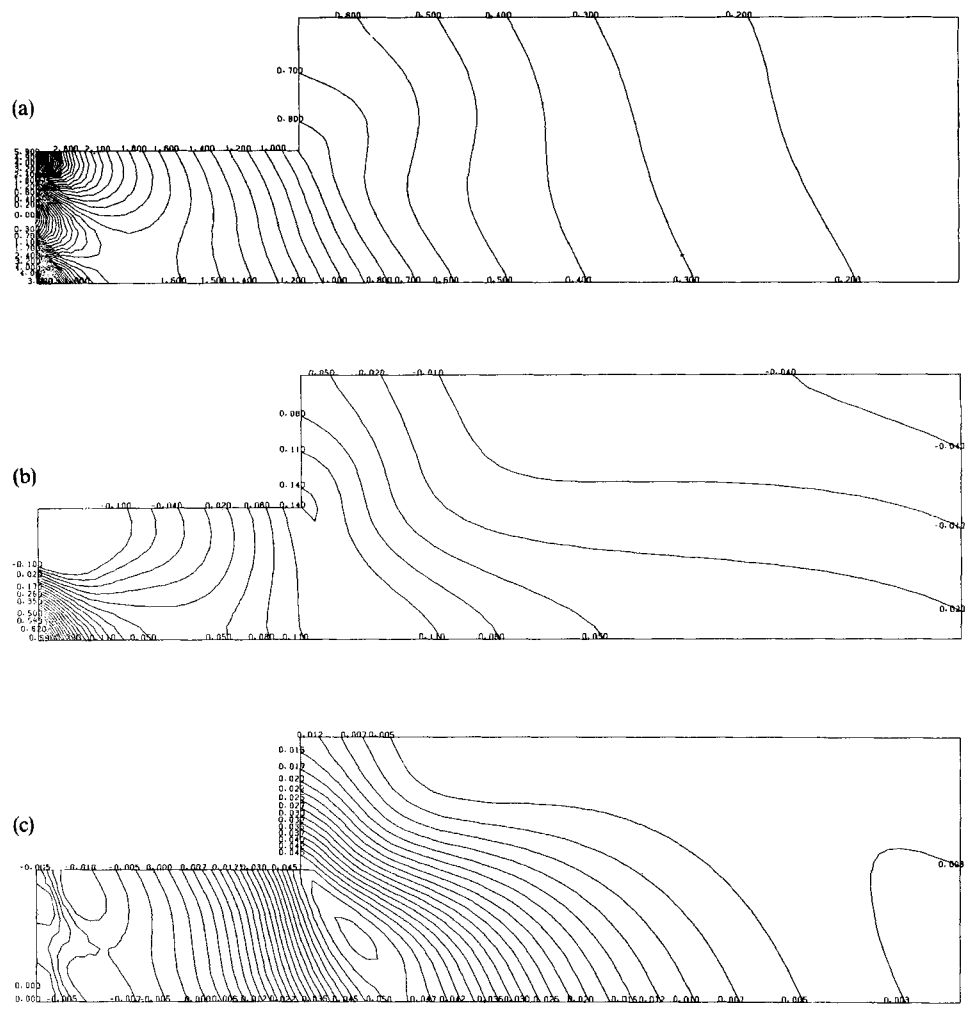

Figure 5. Distribution of extra stress field for $Re=10{\cdot}0$, $We=1{\cdot}0$, $\mu_1=2{\cdot}0$, $\mu_2=1{\cdot}0$, $t=4{\cdot}0$, $\lambda=1{\cdot}0$: (a) extra stress T_{xx}; (b) extra stress T_{xy}; (c) extra stress T_{yy}

CONCLUSIONS

The present numerical analysis investigates the flow of an Oldroyd-B model fluid through a channel with sudden expansion and through a converging–diverging channel. Computational results for velocity, pressure and extra stress fields with different values of Weissenberg number, solvent viscosity and viscosity due to elasticity have been presented. The proper boundary condition for pressure is developed and incorporated in the numerical scheme. It is of interest to point out that the flow of a Maxwell fluid (solvent viscosity $\mu_2=0{\cdot}0$) is a particular case of the present investigation.

For the flow of a Maxwell fluid, it is believed that inclusion of the balancing tensor diffusivity (BTD) technique in the intermediate velocity field and the presence of extra stress gradients and their higher-order derivatives in the exact velocity field and the pressure Poisson equation

Table I. Variation of extra stresses along lower wall ($y=0$, $x>0$) for $Re=10$, $\lambda=1{\cdot}0$

We	μ_2	μ_1	λ_1/λ	Extra stresses	$x=1{\cdot}0$	$x=2{\cdot}0$	$x=3{\cdot}0$	$x=4{\cdot}0$	$x=5{\cdot}0$	$x=6{\cdot}0$	$x=7{\cdot}0$
0·4	1·0	0·1	0·909	T_{xx} %	75·42	82·47	92·31	95·95	96·87	97·25	97·60
				T_{xy} %	86·20	87·73	88·24	91·52	92·42	92·49	93·42
				$T_{yy}\times 10^4$	0·708	10·23	22·95	8·358	1·197	−0·013	−0·127
0·4	1·0	0·5	0·667	T_{xx} %	75·28	82·32	92·02	95·62	96·54	97·00	97·38
				T_{xy} %	86·34	87·78	89·26	91·95	92·45	92·49	93·45
				$T_{xx}\times 10^3$	0·221	5·241	11·53	4·347	0·628	0·040	−0·139
0·4	1·0	1·0	0·500	T_{xx} %	75·17	82·30	91·99	95·50	96·42	96·88	97·25
				T_{xy} %	88·13	89·20	89·34	91·98	92·43	92·51	93·48
				$T_{yy}\times 10^3$	0·354	10·85	22·93	8·664	1·270	−0·015	−0·510
1·0	1·0	1·0	0·500	T_{xx} %	74·78	80·97	89·74	93·43	95·35	96·67	97·14
				T_{xy} %	87·41	88·09	88·81	90·40	91·53	92·12	92·94
				$T_{yy}\times 10^2$	−0·161	1·094	2·251	0·918	0·478	0·205	0·108
2·0	1·0	1·0	0·500	T_{xx} %	72·63	77·00	85·10	88·77	91·54	93·87	95·17
				T_{xy} %	81·39	84·05	86·35	88·97	89·90	91·34	92·68
				$T_{yy}\times 10^2$	0·694	4·672	6·630	3·878	2·195	1·272	0·864
1·0	2·0	1·0	0·667	T_{xx} %	74·63	80·82	89·64	93·36	95·29	96·64	97·03
				T_{xy} %	88·03	89·88	90·12	90·85	92·67	92·74	92·96
				$T_{yy}\times 10^2$	−0·040	1·272	2·573	1·300	0·538	0·242	0·136

Table II. Variation of extra stresses along upper wall ($y=2{\cdot}0$, $x>0$) for $Re=10$, $\lambda=1{\cdot}0$

We	μ_2	μ_1	λ_1/λ	Extra stresses	$x=2{\cdot}0$	$x=3{\cdot}0$	$x=4{\cdot}0$	$x=5{\cdot}0$	$x=6{\cdot}0$	$x=7{\cdot}0$
0·4	1·0	0·1	0·909	T_{xx} %	87·36	94·44	96·84	97·75	98·05	98·03
				T_{xy} %	98·72	98·73	99·20	99·83	99·85	99·92
				$T_{yy}\times 10^5$	22·41	24·91	−0·665	−3·573	−1·668	−0·807
0·4	1·0	0·5	0·667	T_{xx} %	87·12	94·02	96·43	97·42	97·80	97·80
				T_{xy} %	98·76	98·95	99·26	99·85	99·87	99·93
				$T_{yy}\times 10^4$	11·72	12·35	0·322	−1·422	−0·682	−0·131
0·4	1·0	1·0	0·500	T_{xx} %	87·00	93·89	96·30	97·28	97·67	97·69
				T_{xy} %	98·41	98·99	99·34	99·87	99·89	99·94
				$T_{yy}\times 10^3$	2·519	2·853	0·106	−0·282	−0·144	−0·105
1·0	1·0	1·0	0·500	T_{xx} %	85·75	91·06	94·01	95·97	97·14	97·57
				T_{xy} %	96·92	97·05	99·03	99·63	99·62	99·90
				$T_{yy}\times 10^2$	2·028	2·327	0·052	0·166	0·146	0·113
2·0	1·0	1·0	0·500	T_{xx} %	82·81	86·57	89·81	92·65	94·78	95·81
				T_{xy} %	86·32	89·62	93·60	96·61	98·50	98·78
				$T_{yy}\times 10^2$	9·028	9·346	2·546	1·595	1·003	0·758
1·0	2·0	1·0	0·667	T_{xx} %	85·70	90·85	93·88	95·91	97·11	97·55
				T_{xy} %	97·31	98·94	99·89	99·92	99·93	99·93
				$T_{yy}\times 10^2$	2·372	2·516	0·614	0·318	0·174	0·126

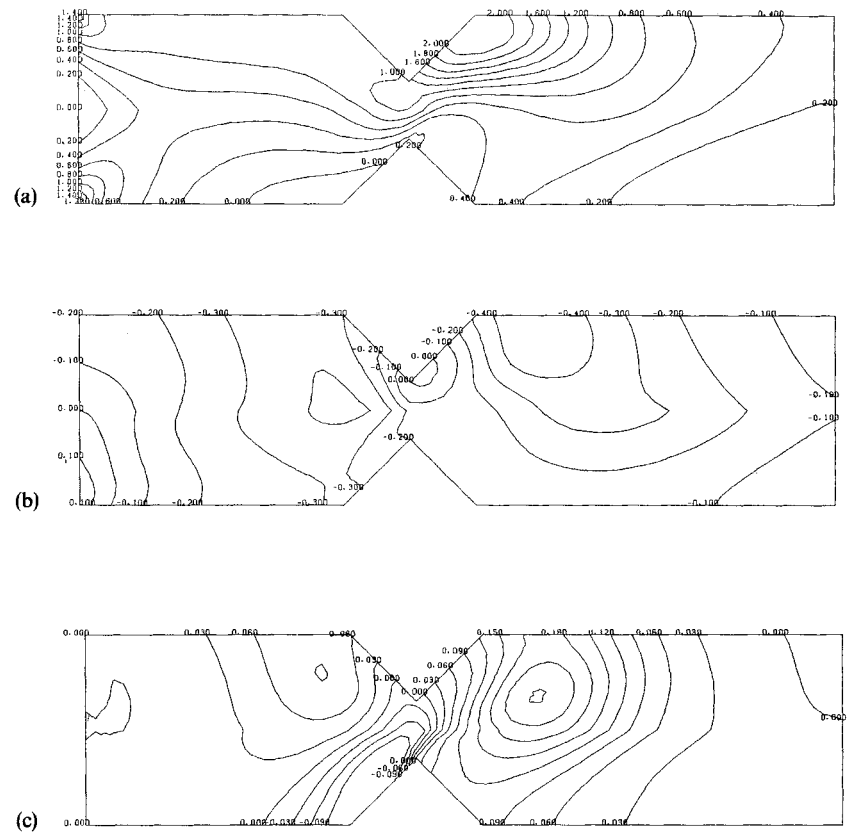

Figure 6. Distribution of extra stress field for $Re = 10{\cdot}0$, $We = 1{\cdot}0$, $\mu_1 = 0{\cdot}5$, $\mu_2 = 1{\cdot}0$, $t = 1{\cdot}0$, $\lambda = 1{\cdot}0$: (a) extra stress T_{xx}; (b) extra stress T_{xy}; (c) extra stress T_{yy}

respectively considerably improve the behaviour of the present algorithm. Furthermore, the presence of second derivatives in the extra stresses in the pressure Poisson equation automatically provides the Neumann boundary condition for the extra stress field if we use a linear interpolation function. A complete analysis of this treatment is under way and will be the subject of a forthcoming paper.

For the first-order forward Euler scheme used in the time integration to analyse unsteady flow, it is observed that convective terms in the momentum and extra stress equations introduce negative viscosity, which ultimately reduces the physical viscosity of the fluid. In order to cancel out the negative viscosity due to the advective terms and obtain more or less exact results of the flow variables, we have to introduce a degree of artificial viscosity into the system of equations through a valid technique. In view of this, BTD and two-step explicit (TSE) techniques in the momentum and extra stress equations respectively have been introduced. It is of importance to note that BTD introduces a little more artificial viscosity than necessary and the accuracy of the computed results is less than that of the TSE method. Furthermore, the BTD technique always provides a stable solution whereas the TSE scheme sometimes may not give a stable solution. Hence the selective-lumping parameter is introduced in order to get a stable solution. It is seen

that the stability and accuracy of the two-step explicit method are dependent not only on the selective-lumping parameter e but also on the time step size, mesh size and other related non-linear factors. It is of interest to point out through an example that for the one-dimensional advection–diffusion flow problem, the artificial viscosity introduced by the two-step explicit scheme is given by $(1{\cdot}0-e)\Delta x^2/6\Delta t$. For a given flow problem and mesh size, the amount of artificial viscosity just to cancel out the negative viscosity is dependent on the parameter e and the time increment Δt. Experience shows that for a small time step size one can choose a large value of the selective-lumping parameter e to compute a stable solution with reasonable accuracy. On the other hand, the value of e must be small if a large time step size has been chosen, otherwise the amount of artificial viscosity could be more than necessary to exactly cancel the negative viscosity. In view of this, $e=0{\cdot}4$, $\Delta t=10^{-3}$, $\Delta x=\Delta y=0{\cdot}1$ have been selected for the fluid flow through a channel with abrupt expansion, and $\Delta x=\Delta y=0{\cdot}05$, $e=0{\cdot}4$, $\Delta t=5{\cdot}10^{-4}$ for the same flow through a channel with converging–diverging cross-section. One of the main questions under investigation is how to derive a formula to compute the proper lumping parameter value along with Δt for a given flow problem with a specific flow geometry and then make a modest effort to generalize the formula. This needs further careful analysis and forms part of our future research.

Finally, it may be said that the present numerical method has successfully demonstrated the applicability of the scheme in analysing the unsteady flow of viscoelastic fluid in different geometries. The numerical method has lessened the problem of storage requirement in comparison with other numerical schemes, and the formulation may be attractive owing to its other advantages. Moreover, use of the present numerical technique for other non-Newtonian fluids flow problems, including the non-isothermal case, solute transport, etc., is deemed promising.

ACKNOWLEDGEMENTS

This research work was supported by the Environmental Research Corporation, Japan. The computation has been carried out using the FACOM VP-30 of Chuo University. One of the authors (R.P.) expresses his gratitude to the students of the Computational Mechanics Laboratory, Chuo University, for their friendly companionship and help, and special thanks to Dr. S. B. Yoon for fruitful discussion.

REFERENCES

1. A. J. Chorin, 'Numerical solution of the Navier–Stokes equations', *Math. Comput.*, **22**, 745–762 (1968).
2. J. Donea, S. Guiliani and H. Laval, 'Finite element solution of the unsteady Navier–Stokes equations by fractional step method', *Comput. Methods Appl. Mech. Eng.*, **30**, 53–73 (1982).
3. J. Donea, S. Guiliani, H. Laval and L. Quartapelle, 'Solution of the unsteady N–S equations by a finite element projection method', in C. Taylor and K. Morgan (eds), *Computational Techniques in Transient and Turbulent Flow*, Pineridge Press, Swansea, 1981.
4. G. E. Schneider and G. D. Raithby, 'Finite element analysis of incompressible fluid flow incorporating equal order pressure and velocity interpolation', in K. Morgan *et al.* (eds), *Computer Methods in Fluids*, Pentech Press, 1980, pp. 49–83.
5. R. Glowinsky, B. Mantel, J. Periaux, P. Perrier and O. Pirronneau. *Proc. on finite elements in fluids*', **4**, 365–401 (1982).
6. M. Kawahara and K. Ohmiya, 'Finite element analysis of density flow using velocity correction method', *Int. j. numer. methods fluids*, **5**, 981–993 (1985).
7. B. Ramaswamy, M. Kawahara and T. Nakayama, 'Lagrangian finite element method for the analysis of two-dimensional sloshing problems', *Int. j. numer. methods fluids*, **6**, 659–670 (1986).
8. B. Ramaswamy, 'Derivation and application of arbitrary Lagrangian Eulerian finite element method for the numerical analysis of nonlinear viscous free surface fluid flow problems', *Ph.D. Thesis*, Chuo University, Tokyo, 1986.
9. M. J. Crochet and K. Walters, 'Numerical methods in non-Newtonian fluid mechanics', *Ann. Rev. Fluid Mech.*, **15**, 241–260 (1983).
10. S. L. Josse and B. A. Finlayson, 'Reflections on the numerical viscoelastic flow problem', *J. Non-Newtonian Fluid Mech.*, **16**, 13–36 (1984).

11. P. Townsend and M. F. Webster, 'An algorithm for the three-dimensional transient simulation of non-Newtonian fluid flows', *Transient/Dynamic Analysis and Constitutive Laws for Engineering Materials, Vol. 2*, 1987, pp. T12/1–11.
12. M. J. Crochet and J. M. Marchal, 'Finite elements for highly viscoelastic flows', *Transient/Dynamic Analysis and Constitutive Laws for Engineering Materials, Vol. 2*, 1987, pp. T53/1–8.
13. P. Townsend, 'Numerical solutions of some unsteady flows of elasticoviscous liquids', *Rheol. Acta*, **12**, 13–18 (1973).
14. J. H. Song and J. Y. Yoo, 'Numerical simulation of viscoelastic flow through sudden contraction using time dependent difference method', in G. Yagawa and S. N. Atluri (eds), *Proc. Int. Natl. Conf. on Computer Mechanics*, Tokyo, 1986, pp. VII: 29–34.
15. J. Y. Yoo and D. D. Joseph, 'Hyperbolicity and change of type in the flow of viscoelastic fluids through channels', *J. Non-Newtonian Fluid Mech.*, **19**, 15–41 (1985).